Scientific paper

Interpreting the Conformational Dynamics Over Interaction of FAM222A Protein with Amyloid-Beta Peptides

Nail Besli¹ , Nilufer Ercin¹ , Miguel Carmena-Bargueño² , Horacio Pérez-Sánchez^{2,*} , Ulkan Celik^{1,3,*}

 1 Department of Medical Biology, Hamidiye School of Medicine, University of Health Sciences, Istanbul, Turkey

² Structural Bioinformatics and High-Performance Computing Research Group (BIO-HPC), Computer Engineering Department, UCAM Universidad Católica de Murcia, Guadalupe, Spain

³ Department of Medical Biology, Institute of Health Sciences, University of Health Sciences, Istanbul, Turkey

* Corresponding author: E-mail: ulkncelik@gmail.com; hperez@ucam.edu

Received: 05-22-2025

Abstract

Alzheimer's disease (AD), a neurological disorder with increasing prevalence worldwide, presents a significant challenge to the medical community. The molecular mechanism underpinning its neuropathology is still wholly unexplained. Recent investigations have focused on the role of the protein aggregatin (AP), encoded by FAM222A, in amyloid-beta (A β) aggregation via its N-terminal A β binding domain. The current study aims to characterize the interaction mechanisms between the AP and A β ($_{1-42 \text{ and } 1-28}$) peptides using all-atom molecular dynamics (MD) simulations. The objective is to assess whether AP is a stabilizing scaffold in A β peptide aggregation, validate docking outcomes from previous studies, and compare the stability and interaction profiles of different A β isoforms. A β ($_{1-42, 1-28}$) peptides were converted from the α -helix to the β -sheet form to inquire better-docked formation with the AP. The selected docking poses from our previous study and the four top scoring from HADDOCK were implemented in MD simulations, resulting in relatively stable complexes as indicated by consistent RMSD/RMSF trends without major structural disruptions. However, no binding free energy or interaction network analysis was conducted, and the conclusions are thus limited to structural stability observations. Our calculations hold accurate points for further experimental AD research on designing and developing the relevant protein-peptide interactions.

Keywords: Aggregatin protein, Amyloid-beta peptide, Alzheimer's disease, Protein-peptide docking, Molecular dynamics simulation

1. Introduction

Alzheimer's disease (AD) is the most common form of dementia worldwide, remaining incurable and continuing to rise in prevalence, primarily due to the aging global population. For many years, the progression of this neurological disorder has been traditionally characterized by the abnormal folding of beta-amyloid peptides, which leads to the formation of plaques alongside the development of neurofibrillary tangles composed of hyperphosphorylated tau protein. An extracellular A β plaque aggregation of protein fibril in abnormal formation is amyloidosis. A β_{1-42} is one of the most toxic pieces of the Amyloid precursor protein (APP) that forms accumulation in the extracellular part. Various models have been proposed to explain fi-

brillation and amyloid-beta $(A\beta)$ aggregation, all of which generally involve structural alterations in the monomeric protein, leading to increased peptide toxicity. These models highlight the transition from native structures to more aggregation-prone forms, which contribute to the pathological effects observed in diseases such as Alzheimer's. Understanding Alzheimer's pathology at an atomic level and how amyloids form stable structures is critical to designing effective therapeutic molecules that could potentially brighten the future of Alzheimer's treatment.

The examination of the impacts of various forms on the structure of $A\beta$ peptides and the comprehension of their toxicity is a prevalent approach for the therapy of AD. However, it has been reported that $A\beta$ peptide aggregation processes are linked to multiple factors, including muta-

tion, alterations in species concentration, and low variation in physiological conditions, the proportion of $A\beta_{1-40}$ to $A\beta_{1-42}$, and generate alternative structures for the peptide. This disarrangement of the peptide structure, linked with a broad range of complex structures, has conducted not only experimental approaches adequate to investigate the beta-amyloid peptide structure but plenty of computational studies have been performed in this field.⁶⁻⁸ From one of the experimental and hypothetical works, a number of researchers have recently discovered that the protein Aggregatin (AP) encoded by FAM222A (Family with sequence similarity 222 member A) interacts with $A\beta_{1-42}$ peptide by its N-terminal Aß binding domain and its characteristic accumulation in the heart of AB plaques. Accordingly, the results have exhibited the protein that may play a critical role in amyloidosis by facilitating Aß aggregation.9 In one of our former studies, we conducted the first structural biology investigation following the discovery of the AP and revealed interaction poses with the Aβ peptide. 10 Plus, another study showed that FDA-approved drugs could target AP by identifying it as a potential drug target and providing a beacon of hope in triggering in vitro

and in vivo assays for the battle against AD.¹¹ The central hypothesis of this study is that AP facilitates A β aggregation by acting as a stabilizing scaffold, particularly through interactions with the N-terminal regions of A β peptides. To test this, we performed all-atom MD simulations on previously docked complexes of AP with A β ₁₋₂₈ and A β ₁₋₄₂, aiming to evaluate interaction strength, structural stability, and isoform-specific differences.

In the prevailing study, we have subjected the molecular dynamics (MD) simulation of the docking complexes of the AP with A β peptides (A β_{1^-42} , A β_{1^-28}) using various computational approaches in our previous paper. ¹⁰ Besides, we analyzed the features of the sequences and functional annotations of the amyloid beta-peptide sequence in the primer structure of the APP. This study highlights the relatively unexplored interaction between aggregation and the A β analysis over the MD simulation. The former docking analysis identified this interaction, and the outcomes were confirmed with MD simulations. This extensive study uses the predicted structure of FAM222A protein to stimulate the interaction, which stays profoundly stable through the MD analysis.

Aggregatin protein facilitates Aβ aggregation

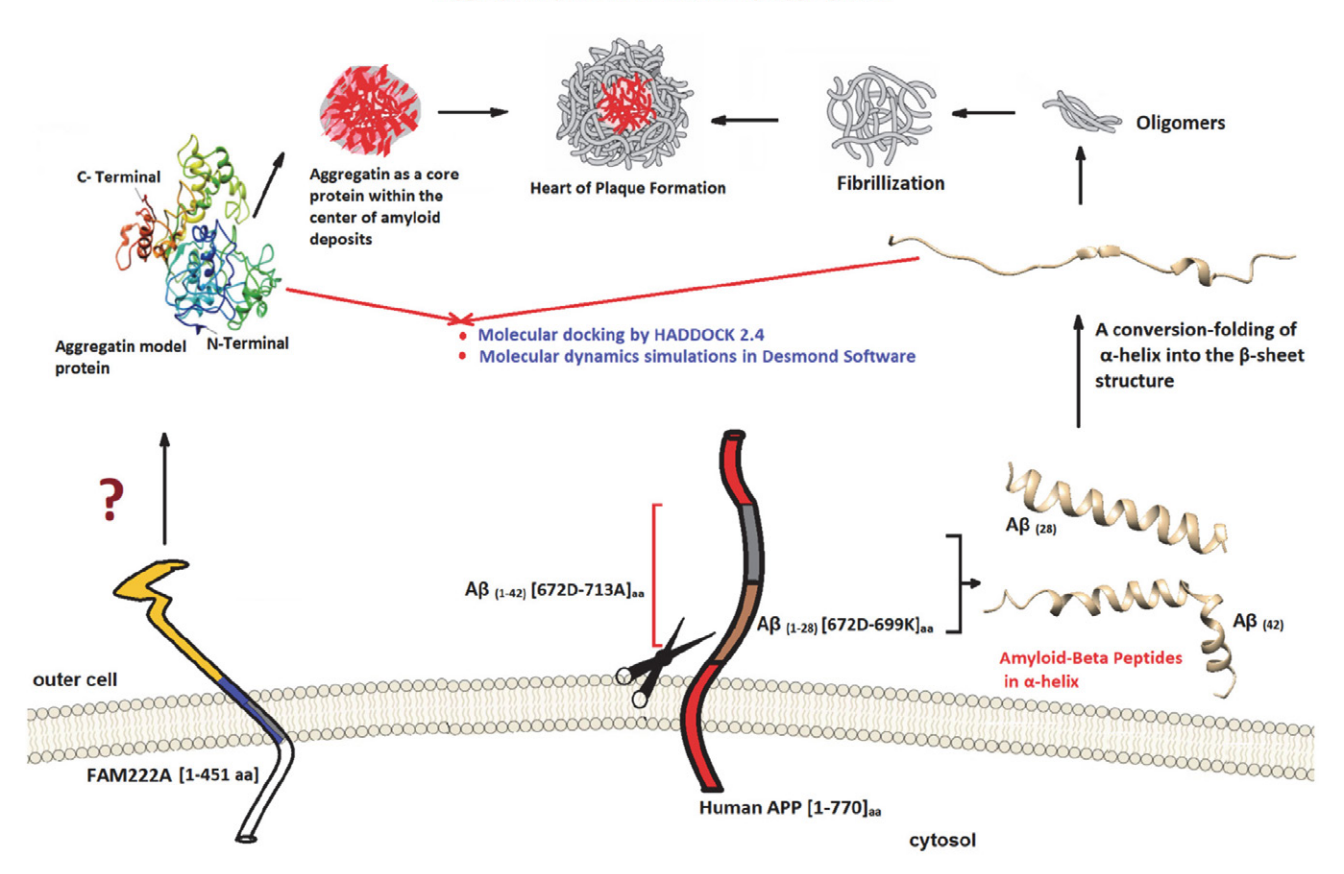


Figure 1: Schematic representation of the proposed role of Aggregatin (AP) in facilitating $A\beta$ peptide aggregation. The illustration shows AP localized at the cell membrane, where its interaction with extracellular $A\beta$ peptides ($A\beta_{1^-28}$ and $A\beta_{1^-42}$) may promote β-sheet conversion and nucleation. The diagram highlights the N-terminal $A\beta$ binding domain of AP and its potential scaffolding function in amyloid plaque formation, as suggested by MD simulations and prior localization studies. AP: Aggregatin protein, $A\beta$: Amyloid-beta peptide, MD: molecular dynamics.

2. Materials and Methods

2. 1. Protein and Peptide Preparation for Molecular Docking Simulations

Although our previous study¹⁰ presents the full pipeline in detail, for clarity and continuity we briefly summarize the approach here. The AP structure (encoded by FA-M222A) was modeled via homology modeling due to the absence of a crystallized structure. Secondary structure prediction was first performed using PSIPRED¹², followed by tertiary structure generation using the Robetta server.¹³ Energy minimization of the AP and Aβ peptide structures was carried out using UCSF Chimera with 1000 steepest descent steps followed by 100 conjugate gradient steps, employing the default AMBER force field within Chimera. The aim was to relieve steric clashes and optimize geometry prior to docking. A β peptides (1AMB for A β_{1-28} and 1IYT for $A\beta_{1-42}$) were retrieved from the RCSB Protein Data Bank and prepared similarly. Moreover, the Aβ peptides were initially evaluated using PSIPRED to predict their secondary structural tendencies. Consistent with prior findings in AD research, both $A\beta_{1-28}$ and $A\beta_{1-42}$ showed β-sheet-dominant secondary structures in the prediction stage. These predicted conformations were then used to model the 3D structures, which allowed us to simulate a physiologically relevant aggregation-prone state, rather than the native α -helical monomeric form. Our objective was to capture interaction dynamics under conditions that closely mimic the pathological β-sheet transition known to precede fibril formation. Docking was subsequently carried out using HADDOCK 2.414, and selected top-ranked poses were further subjected to all-atom MD simulations using Desmond.

For the preparation of docking process, we removed the water, added the polar hydrogen to the model protein. Then, we charged the model protein and the peptides by the computation of Gasteiger using AutoDock Vina. ¹⁵ Prior to performing the docking process, the energy minimization and refinement of 3D model protein structure was performed using underwent energy minimization by Chimera 1.14. ¹⁶

2. 2. Protein-Peptide Docking Process

All protein-peptide interaction clusters were obtained in the last stage by automatizing HADDOCK 2.4.¹⁴ By default, HADDOCK 2.4 executes the cluster and model analysis. This model was evaluated based on the HADDOCK score and Z-score, with 0.6 as the cutoff and 4 as the minimum cluster size. HADDOCK's scoring function integrates energies and buried surface area for different docking stages: rigid body (it0), semi-flexible refinement (it1), and explicit solvent refinement (water).¹⁴ The z-score accurately indicates the number of standard deviations that distinguish the HADDOCK score of a specific cluster from the mean of all clusters.^{14,17} The complexes were,

therefore, ranked based on the average HADDOCK score and Z-score. In the submission to HADDOCK, the proline-riched region in the AP protein and the N-terminal region of AB peptides were prioritized as active residues, causing the docking results more reliable. The proline-rich region of AP (residues 147-299) was selected based on our previous study identifying its surface exposure and sequence flexibility. Moreover, literature suggests that proline-rich domains are inv olved in protein-protein interactions, especially in neurodegenerative diseases.¹⁸ The N-terminal residues of $A\beta_{1-28}$ were prioritized based on previous experimental findings showing that this region mediates aggregation propensity and initiates early interactions during fibril formation.^{9,19} Therefore, active residues were chosen based on both structural features and biological relevance. The grid box was automatically arranged to cover these residues, assuring they were entirely covered. The process of automatically placing passive residues around the active ones has been defined. The minimum relative solvent accessibility (RSA) for active residues is confidently set at 15%, whereas passive surface neighbors maintain a minimum RSA of 40%. HADDOCK 2.4 conducted a cluster and model analysis with the default settings. The force constant for the center of mass contact and surface contact restraints was set to one for distance restraints. Random exclusion had two sections, and the gyration radius was 17.78. The sample parameters were fine-tuned by utilizing 1000 configurations for rigid body docking, followed by five rounds of rigid body minimization, and 200 configurations were further refined in a semi-flexible manner, 200 models were utilized for the final stages of refinement and evaluation. The docking outcomes were clustered using the Fraction of Common Contacts (FCC) method, applying a root mean square deviation (RMSD) threshold of 0.6 and a minimum cluster size of 4. Regarding analysis parameters, hydrogen bonds were defined with a distance cutoff of 3.5 Å between proton donors and acceptors, while hydrophobic interactions between carbon atoms were characterized using a 3.9 Å cutoff. Clusters with lower Z-scores indicated higher confidence in the docking results. For docking pose selection, HADDOCK-generated clusters were ranked based on HADDOCK score, cluster size, and Z-score. Only poses from top-ranked clusters (Z-score<-1.5, cluster size≥4) were considered. Among these, representative structures were selected for MD simulations based on their buried surface area and electrostatic complementarity. In total, six distinct complexes covering diverse interaction orientations were chosen for further analysis.

2. 3. Molecular Dynamics (MD) Simulations

To assess the structural stability and confirm the static interactions between AP and $A\beta_{(1-28,\ 1-42)}$ peptides, MD simulations were implemented using the Desmond Software.²⁰ The dynamic behavior of protein-peptide in-

teractions was explored at an atomic level. The protein-peptide complexes were placed in a solvated box containing water and sodium ions (Na+) to neutralize the system. Specifically, the Aggregatin-Aβ₁₋₄₂ complex comprised ~6,600 atoms (452 residues) before solvation, increasing to 52,557 atoms after addition of 15,075 SPC water molecules and 99 counter-ions (57 Cl-, 42 Na+). The Aggregatin-Aβ₁₋₂₈ complex similarly comprised ~6,600 atoms before solvation, increasing to 59,663 atoms after addition of 17,502 waters and 113 counter-ions (64 Cl-, 49 Na⁺). A Simple Point Charge (SPC) water model was applied, with the box dimensions set at 10 Å \times 10 Å \times 10 Å. The SPC water model was chosen for its compatibility with the OPLS3e force field implemented in the Desmond software suite, as well as its computational efficiency in largescale protein-peptide simulations. Previous MD studies on similar peptide aggregation systems have successfully employed SPC, showing reliable structural dynamics.²¹ Although TIP3P and TIP4P are more frequently used in studies focusing on detailed hydrogen bonding and solvation effects, SPC remains a widely accepted model in scenarios where computational performance is prioritized. We acknowledge that water model selection can influence protein-water hydrogen bonding patterns, dielectric properties, and peptide flexibility. As a future direction, we plan to perform comparative simulations using TIP3P to validate that the key interaction trends and overall structural stability of AP-AB complexes are conserved regardless of the water model applied. Energy minimization was achieved using the steepest descent method for 2000 steps, applying a threshold of 1.0 kcal/mol/Å. Simulations were conducted under NPT conditions at 300 K and 1 bar, regulated by the Martyna-Tobias-Kleina barostat and Nosé-Hoover thermostat algorithms. 22-24 Each simulation ran for 100 ns, with periodic boundary conditions applied. A 2 femtosecond (fs) timestep was employed throughout all simulations, which is a standard value for all-atom biomolecular dynamics with the OPLS3e force field. Although each simulation was limited to 100 ns, we emphasize that multiple docking poses were simulated independently across both $A\beta_{1^{-}28}$ and $A\beta_{1^{-}42}$ peptides. These simulations explored different initial binding configurations of the same AP protein, thereby offering a comparative view across structurally distinct complexes. While longer trajectories (e.g., 500 ns) could offer further insights into rare conformational transitions, the current approach enables effective assessment of structural stability and relative binding trends across multiple replicates. Future work may investigate extended trajectories for one representative system to confirm long-term behavior. For van der Waals interactions, a 9 Å cutoff was employed, while electrostatic interactions were handled using the Particle Mesh Ewald (PME) method with a tolerance of 10^-9. The OPLS3e force field was utilized throughout the simulations.²⁵ Metrics from the MD simulations, including RMSD and rootmean-square fluctuation (RMSF), were calculated using

the Simulation Interaction Diagram (SID) and prime software from the Maestro-Suite. These tools evaluate how the overall structure (RMSD) and individual residues (RMSF) evolve over the 100 ns simulation by comparing each frame with the initial structure. Finally, the dynamic properties of protein-peptide interactions were also analyzed at an atomic level to gain further insight into their interaction patterns.

3. Results and Discussion

It has been stated that AP facilitates A β aggregation by physically interacting with A β and thus accumulates at a high rate in the center of amyloid plaques. Since reducing AP accumulation is seen as a therapeutic approach to preventing the progression of AD, it is imperative to reveal the interaction between AP and A β peptides. ²⁶ In the current paper, MD simulations were performed on the structures of A β _(1-28, 1-42) peptide and AP for 100 ns, and we detected stabilization at the atomic level.

3. 1. Evaluation of Amyloid-Beta Protein Structure

In Figure 2, the joint regions and sequence features of protein residues of $A\beta_{1-28}$ (PDB:1AMB) and $A\beta_{1-42}$ (PDB:1IYT) obtained from Uniport were shown by Jalview 2.12 visualization.²⁷ The APP was used as a reference to determine the amyloid sequence features. 676, 681, 684, 695, 704, and 706 residue numbers represent mutagenesis sites, which are crucial for understanding the impact of mutations on protein structure and function. It shows 672, 673, 688, 691, 704, 706, 712, 713 site types, which are important for identifying the specific characteristics of each site. The residue range 695 and 722 has been determined as the region of interest. Residues 677-680 and 695-698 represent rotation in the secondary structure; Residues 683-685, 688-691, 701-703, 707-712 represent the strand in the secondary structure, and 675-675, 713-715 represent the helix in the secondary structure. Residues 18–701 indicate the topological domain in the extracellular area, 702-722 indicate the transmembrane region, residues 677, 681, 684, and 685 indicate the metal ion-binding region, and 681 indicate the glycosylation region (as shown in Tablo 1). Two regions of Aβ, K16-E22 residues (represented here, K687-E693) and K28-G38 (K699-V709), form hydrophobic pockets with hydropathy characteristics. These regions are likely to interact hydrophobically with AP.

3. 2. Assessment of Molecular Dynamics Outcomes

RMSD analysis reveals the structural deviations of entire protein molecules over time. The RMSF plot

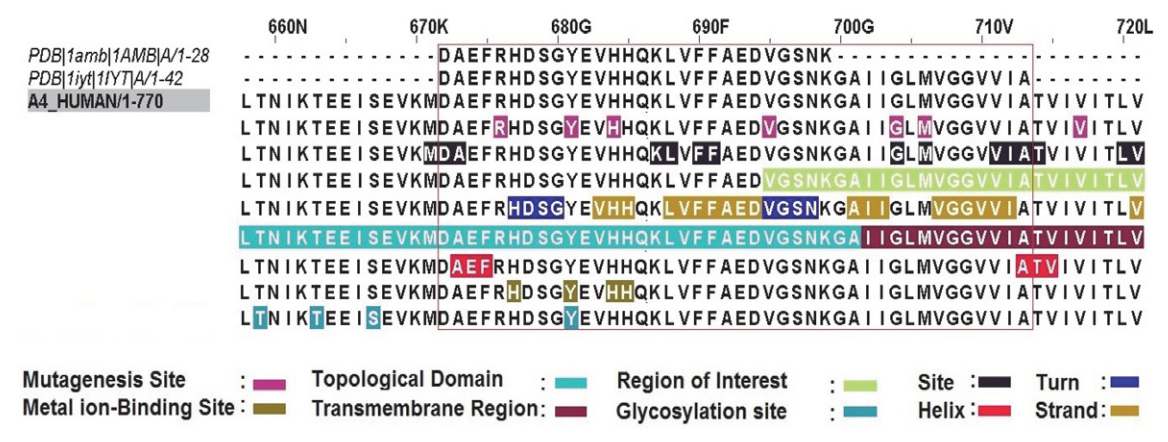


Figure 2: Visualization of key sequence features of the APP (UniProt ID: P05067), highlighting residue annotations derived from $A\beta_{1-28}$ (PDB: 1AMB) and $A\beta_{1-42}$ (PDB: 1IYT). The displayed region includes known cleavage sites, mutagenesis hotspots, secondary structure elements, and metal-binding residues. The APP sequence was used as a reference for alignment, and only the common residues among APP, $A\beta_{1-28}$, and $A\beta_{1-42}$ are shown. Color coding reflects annotated structural or functional features. APP: amyloid-beta precursor protein, $A\beta$: Amyloid-beta peptide, PDB: protein data bank

Table 1: A list of sequence features (the range of 672–713) for amyloid-beta precursor protein was retrieved from Uniprot database ²⁸ using Jalview 2.12

Т	Sequence Feature Details (672-713)	D ! J
Туре	Description	Residue no.
Mutagenesis site	Arg676Gly 60-70% zinc-induced amyloid-beta protein 28 aggregation	676
	Tyr681Phe 60-70% zinc-induced amyloid-beta protein 28 aggregation	681
	His684Arg Only 23% zinc-induced amyloid-beta protein 28 aggregation	684
	Val695Cys Causes formation of an artefactual disulfide bond with PSEN1.	695
	Gly704Val Reduced protein oxidation. No hippocampal neuron toxicity	704
	Met706Leu Reduced lipid peroxidation inhibition. Met706Val No free radical production. No hippocampal neuron	706
Site	Cleavage; by beta-secretase 671–672,	672
	Cleavage; by caspase-6; when associated with variant 670-N-L-671	673
	Cleavage; by alpha-secretase(687–688)	688
	Cleavage; by theta-secretase(690–691)	691
	Implicated in free radical propagation	704
	Susceptible to oxidation	706
	Cleavage; by gamma-secretase; site 1(712–713)	712
	Cleavage; by gamma-secretase; site 2(713–714)	713
Region of Interest	Interaction with PSEN1	695-722
Turn	Secondary structures	677-680
	•	695-698
Strand	Secondary structures	683-685
	,	688-691
		701-703
		707-712
Topological Domain	Extracellular region	18-701
Transmembrane Region	Helical	702-722
Helix	Secondary structures	675–675
	,	713-715
Metal ion-Binding site	Copper or zinc 2	677
		681
		684
		685
Glycosylation site	O-linked (HexNAc) tyrosine; partial	681

quantifies the average positional deviations of individual residues over the course of the simulation, reflecting their local flexibility. Higher RMSF values typically correspond to loop regions or solvent-exposed termini, while lower values indicate structurally stable or buried segments. In the context of protein-peptide MD simulations, an RMSD range of 2–4 Å is generally considered indicative of structural stability, whereas sustained deviations beyond 5 Å may suggest significant conformational drift. Similarly, RMSF values under 2.0 Å typically

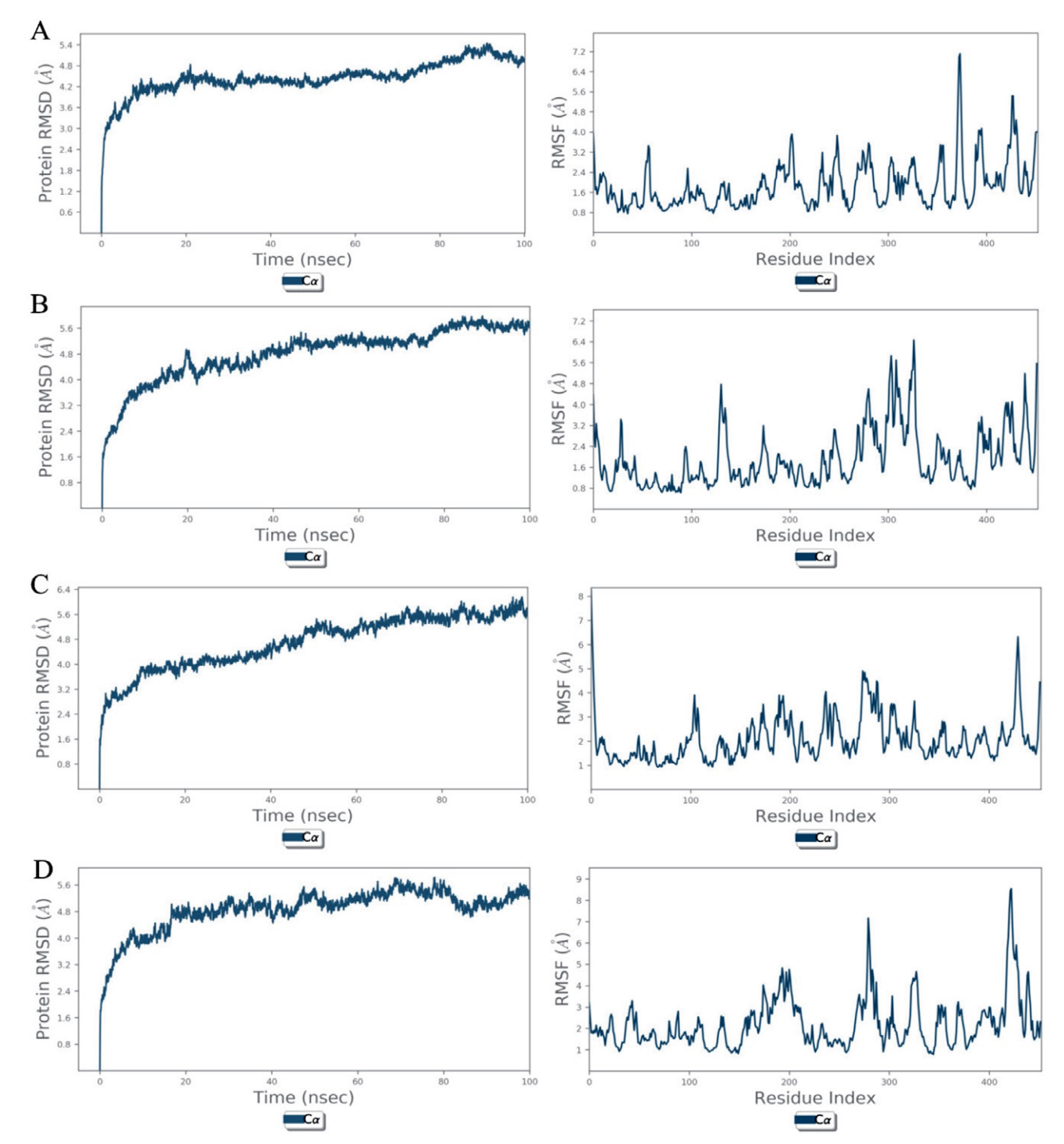


Figure 3: RMSD and RMSF plots illustrating the structural stability and residue-level flexibility of AP-A $β_{1-42}$ complexes over 100 ns MD simulations. Each panel represents a distinct docking complex generated using HADDOCK, labeled as FREEDOCK1_C, IES1_A, IES6_B, etc., reflecting different binding poses and interaction surfaces. Left panels display the RMSD of backbone atoms, indicating overall conformational drift, while right panels show the RMSF of individual residues, highlighting flexible loop regions and stable core domains. Comparisons across docking configurations reveal that all complexes reached stable RMSD plateaus within the first 30–40 ns, and that the proline-rich region of AP and the central region of Aβ contributed most to sustained interactions. AP: Aggregatin protein, Aβ: Amyloid-beta peptide, MD: molecular dynamics, RMSD: root mean square deviation, RMSF: root-mean-square fluctuation.

correspond to rigid, well-structured regions, while higher fluctuations (above 5.0 Å) are often observed in flexible loops or disordered termini. These thresholds were used as reference points to assess the relative stability and flexibility of the AP-AB complexes. Furthermore, when comparing the different AP-A β complexes, A β_{1-28} complexes generally exhibited lower RMSD fluctuations (~2.5-3.5 Å) and more consistent structural convergence compared to A\(\beta_{1-42}\) complexes, which showed slightly higher deviations (~3.5-5.0 Å). This may be attributed to the additional C-terminal residues in $A\beta_{1-42}$ that contribute to increased flexibility and surface exposure. RMSF profiles also revealed that loop regions and termini were consistently the most dynamic in both complexes, but the magnitude of fluctuation was more pronounced in $A\beta_{1^{-}42}$ systems. Despite these differences, all complexes retained stable backbone conformations and persistent AP-A β contacts throughout the simulation window.

The complex labels such as "FREEDOCK1_C", "IES1_A", and "IES6_B" refer to top-scoring docking poses identified in our previous study 10 , where both FreeDock and HADDOCK 2.4 platforms were used to model the AP-A β interactions. These docking-derived poses were selected based on HADDOCK scores, Z-scores, and cluster rankings, and were carried forward into the present study for MD simulations to assess their structural stability and dynamic behavior. The nomenclature has been preserved to ensure continuity and traceability between the docking and simulation phases.

Figure 3 displays the RMSD and RMSF graphs from MD simulations of the potential complexes of AP and A β_{1-42} obtained from FREEDOCK and IES. The RMSD plots in Figure 3-A, B, C, and D showed small fluctuations up to 5.4

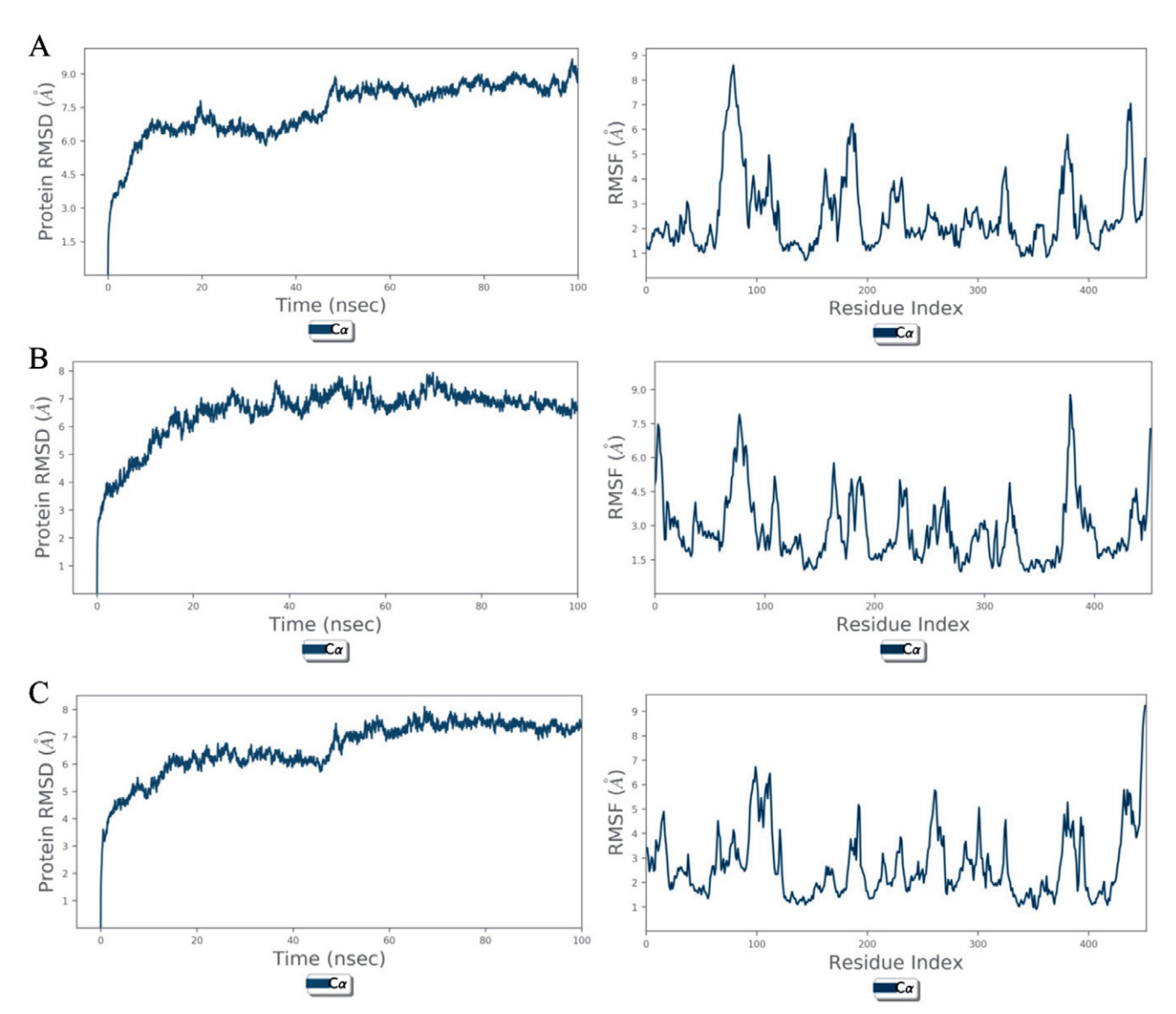


Figure 4: Analysis of the results of the MD simulation of complexes of AP and $A\beta_{1-28}$. A) $A\beta_{1-28}$ FREEDOCK2_A Docking Complex B) $A\beta_{1-28}$ FREEDOCK4_B Docking Complex C) $A\beta_{1-28}$ FREEDOCK8_C Docking Complex. AP: Aggregatin protein, A β : Amyloid-beta peptide, MD: molecular dynamics.

Å, 5.6 Å, 6.0 Å, and 6.4 Å, respectively, while exhibiting relatively stable changes throughout the 100 ns simulation. The RMSD values in Figure 3-A, B, C, and D range from 3.0 to 4.2 Å, 1.6 to 4.8 Å, 2.4 to 5.0 Å, and 2.0 to 4.8 Å, respectively. In Figures 3-A, B, C, and D, the protein's RMSF shows that the average fluctuation of residues ranges from

0.8 to 7.2 Å, 0.8 to 6.4 Å, 1.0 to 8.0 Å, and 1.0 to 8.0 Å, respectively. It's worth noting that secondary structural elements such as alpha helices and beta strands, being more stable, exhibit less fluctuation compared to unstructured parts of the protein.²¹ In the RMSF plot shown in Figures 3-A, B, C, and D, fluctuations were observed in regions out-

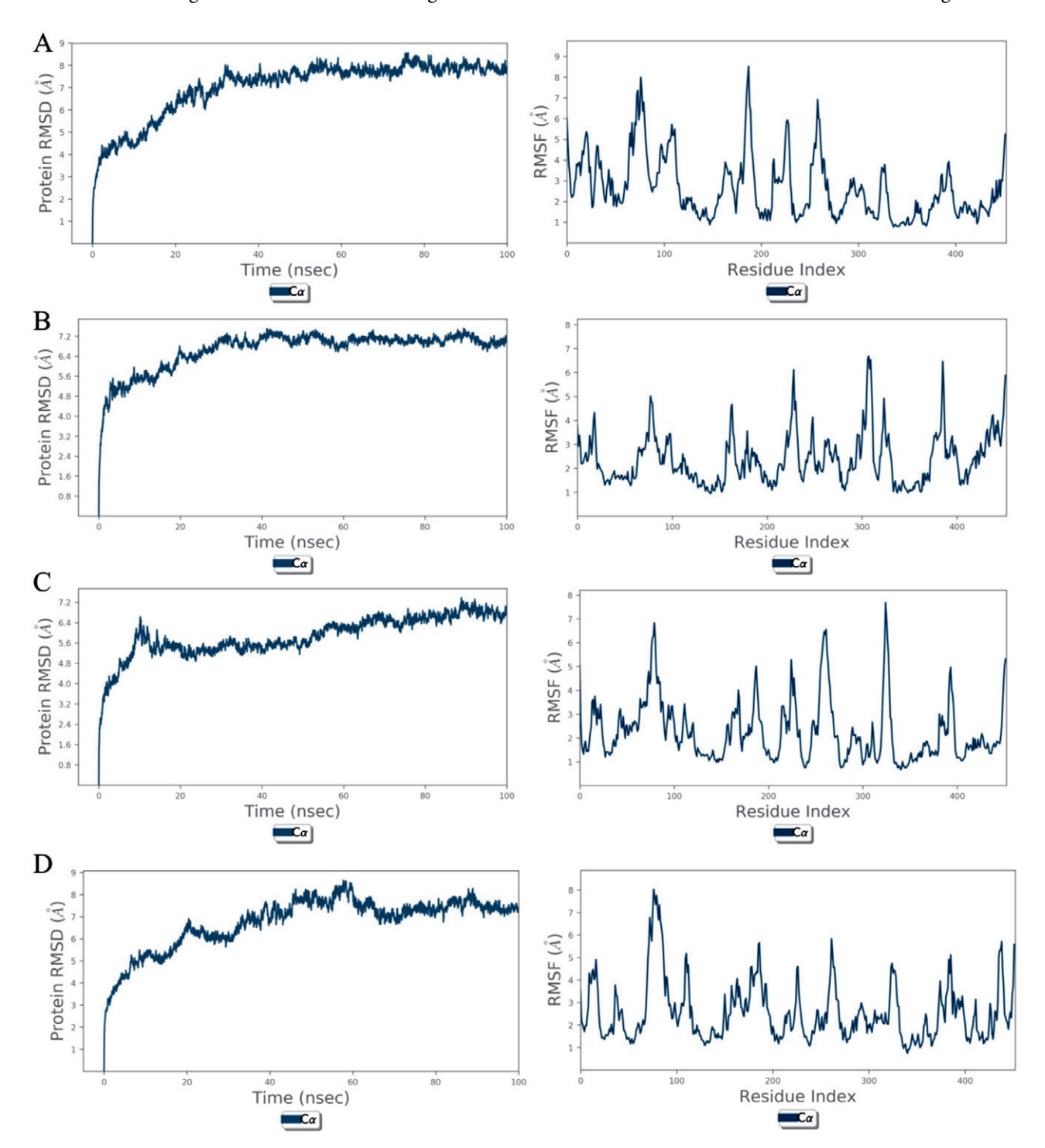


Figure 5: Analysis of the results of the MD simulation of complexes of AP and $A\beta_{1-28}$. A) $A\beta_{1-28}$ SOAP_A₁ Docking Complex, B) $A\beta_{1-28}$ SOAP_A₂ Docking Complex C) $A\beta_{1-28}$ IES2_B₁ Docking Complex D) $A\beta_{1-28}$ IES2_B₂ Docking Complex. AP: Aggregatin protein, A β : Amyloid-beta peptide, MD: molecular dynamics.

side of secondary structural elements such as alpha helices and beta strands (see Supplementary file 1). Similar and relatively stable changes were observed in all complexes.

Figure 4 displays the RMSD and RMSF graphs from MD simulations of the potential complexes of AP and Aβ₁₋₂₈ obtained from FREEDOCK. The RMSD plots in Figure 4-A, B and C showed small fluctuations up to 9.0 Å, 8.0 Å and 8.0 Å, respectively, while exhibiting relatively stable changes throughout the 100 ns simulation. The RMSD values in Figure 4-A, B and C range from 3.5 to 8.0 Å, 3.5 to 6.5 Å and 3.5 to 7.0 Å, respectively. In Figure 4-A, B and C the protein's RMSF shows that the average fluctuation of residues ranges from 1.0 to 8.5 Å, 1.5 to 8.5 Å and 1.0 to 9.0 Å, respectively. In the RMSF plots of Figure 4-A, B and C, fluctuations were observed in the regions outside the secondary structural elements (see Supplementary file 1). When all complexes were evaluated, a similar and relatively stable structure was not observed.

Figure 5 displays the RMSD and RMSF graphs from MD simulations of the potential complexes of AP and $A\beta_{1-28}$ obtained from SOAP and IES. The RMSD plots in Figure 5-A, B, C and D showed small fluctuations up to 8.5 Å, 7.2 Å, 7.2 Å, and 8.5 Å, respectively, while exhibiting relatively stable changes throughout the 100 ns simulation. The RMSD values in Figure 5-A, B, C and D range from 4.0 to 7.5 Å, 4.5 to 7.0 Å, 3.5 to 6.5 Å, and 3.0 to 7.0 Å, respectively. In Figure 5-A, B, C and D, the protein's RMSF shows that the average fluctuation of residues ranges from 1.0 to 8.5 Å, 1.0 to 7.0 Å, 1.0 to 8.0 Å, and 1.0 to 8.0 Å, respectively. In the RMSF plot shown in Figure 5-A, B, C and D, fluctuations were noted in areas outside the secondary structural elements, including alpha helices and beta strands (see Supplementary file 1). Similar and relatively stable structures were observed in complexes. Consequently, MD results of the possible complexes between AP and A β suggest that AP forms a more stable structure with $A\beta_{1-42}$ compared to $A\beta_{1-28}$.

Although certain trajectories reached RMSD values as high as 8-9 Å, RMSF profiles clarified that these deviations primarily originated from flexible loop and terminal regions, rather than disruption of the binding interface. Notably, the interface residues of AP (P185, G186, N195) and A β (H13, K16) consistently maintained low RMSF values, reflecting conformational rigidity at the binding site. This indicates that elevated RMSD values in some complexes reflect localized flexibility rather than global structural instability

HADDOCK 2.4 ranks the top clusters as the most dependable, delivering optimal outcomes in Figure 6-A and B. Considering the cluster scores and their standard deviations, the highest-ranking cluster is identified by its Z-score, where a more negative Z-score indicates significantly higher accuracy compared to the second-ranked cluster. When the Z-scores of different clusters vary by a standard deviation, each cluster should be treated as a viable solution for docking. Additionally, independent exper-

imental data should be used to confirm the optimal solution. In the docking complex, polar interactions are established between residues from AP and the N-terminal region of AB peptides. As results in the Figure 6, the Z-score is –2.0 in the cluster of AP and A β_{1-28} , while the cluster of AP and A β_{1-42} has –2.2 in A. In the B section, the cluster of AP and A β_{1-28} is –1.6 whereas the cluster of AP (targeting to proline-riched region) and A β_{1-42} is –1.8 in A section.

To complement the dynamic analyses, representative structural snapshots of the Aggregatin-Aβ complexes were generated (Figure 6). Both $A\beta_{1-28}$ and $A\beta_{1-42}$ peptides were observed to engage the proline-rich domain (PRD) of AP through a network of hydrogen bonds and polar contacts. In the AP-A $\beta_{1^{-}42}$ complex (Figure 6A), residues H13, K16, and L34 of Aβ formed stable hydrogen bonds with G186, P185, Q205, and N195 of Aggregatin, maintaining persistent contacts throughout the simulation. In the AP-A β_{1-28} complex (Figure 6B), interactions were dominated by H6, H13, and K16 of AB with P168, P235, and S281 of Aggregatin, contributing to a more compact and rigid binding mode. These structural observations corroborate the RMSD and RMSF results, which indicated that $A\beta_{1-28}$ forms more stable contacts at the PRD, while $A\beta_{1-42}$ exhibits a more dynamic binding pattern consistent with its higher intrinsic flexibility.

A comparative analysis of RMSF profiles further revealed distinct patterns of flexibility between the two simulated systems. In AP-A β_{1-28} complexes, fluctuations were largely confined to N-terminal loops and solvent-exposed segments, whereas residues at the binding interface remained stable with RMSF values typically between 2-4 Å. In contrast, AP-Aβ₁₋₄₂ complexes displayed broader fluctuation peaks, particularly in the C-terminal region, with values exceeding 6 Å at multiple positions. Importantly, residues involved in persistent hydrogen bonding, such as H13 and K16 of A\(\beta\) and P185, G186, and N195 of Aggregatin, corresponded to regions of low RMSF, underscoring their contribution to interface stability. These results align with the RMSD trajectories, which plateaued after 30-40 ns, indicating that local flexibility did not compromise the global stability of the complexes.

In the Figure 7A, the measured distances between the center of mass of AP and A β peptides (A β_{1-28} and A β_{1-42}) show consistent fluctuations over time, indicating the dynamic interaction between the two molecules. The Protein-Ligand RMSD plot demonstrates stability, with RMSD values showing limited deviation from the initial distance between the AP and A β peptides. The stability is further confirmed by the RMSF plot, which shows relatively low fluctuations across the protein residues, suggesting that the binding interaction does not induce significant structural changes in AP, particularly in its interaction with both A β_{1-28} and A β_{1-42} .

In the Figure 7B, the focus on the proline-rich region of AP in the Protein-Ligand RMSD and RMSF plots shows

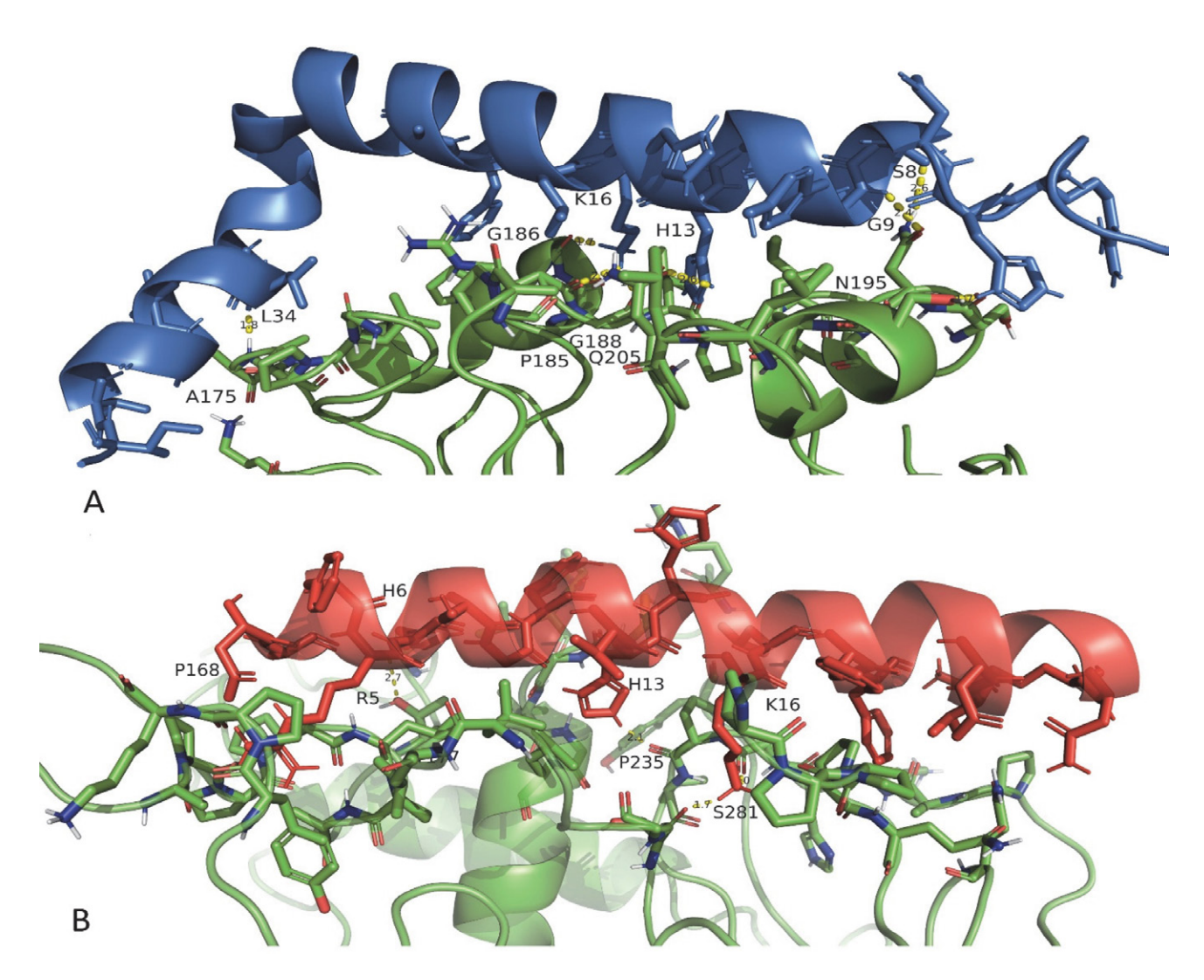


Figure 6: Structural representations of AP-Aβ complexes highlighting the proline-rich domain binding interface. (A) AP (green) bound to $A\beta_{1-42}$ (blue). (B) AP (green) bound to $A\beta_{1-28}$ (red). In both complexes, hydrogen bonds and polar contacts at the protein–peptide interface are shown as yellow dashed lines, with interacting residues displayed in stick representation and labeled. Key interactions involve Aβ residues (e.g., H13, K16, L34 for $A\beta_{1-42}$; H6, H13, K16 for $A\beta_{1-28}$) forming persistent hydrogen bonds with AP residues (e.g., G186, P185, Q205, N195, P235, S281). These structural snapshots illustrate how both Aβ isoforms establish stable contacts with the proline-rich domain of Aggregatin, with $A\beta_{1-28}$ displaying a more compact interaction compared to the more dynamic $A\beta_{1-42}$ complex, consistent with RMSD/RMSF analyses. AP: Aggregatin protein, Aβ: Amyloid-beta peptide, RMSD: root mean square deviation, RMSF: root-mean-square fluctuation.

similar patterns of stability, with RMSD values slightly higher than in the general interaction analysis. The proline-rich region's flexibility contributes to minor fluctuations, but the overall binding remains stable. The RMSF plot highlights some regions of higher mobility, potentially corresponding to regions involved in flexible loop regions of AP, but these fluctuations do not significantly impact the global stability of the AP-A β complex. These results suggest that AP's binding to A β peptides, particularly within its proline-rich regions, is stable and does not induce significant conformational instability. The steady RMSD values reinforce the idea that AP can maintain its structural integrity while interacting with amyloid-beta, a critical factor in promoting amyloid aggregation.

To further evaluate the persistence of peptide-protein interactions, we monitored the center-of-mass (COM) distances between AP and A β isoforms over the 100 ns trajectories (Figure 7). For both A β_{1-28} and A β_{1-42} , the global Aggregatin-A β COM distances remained within 3–6 Å, confirming stable overall association (Figure 7A). However, when focusing specifically on the proline-rich domain (PRD) of Aggregatin, distinct behaviors were observed between the two isoforms (Figure 7B). A β_{1-28} maintained a compact and stable interaction (~5 Å) throughout the trajectory, whereas A β_{1-42} displayed larger fluctuations and progressively drifted beyond 8 Å after ~60 ns. These results indicate that while both peptides stably associate with Aggregatin, the shorter A β_{1-28} isoform forms a more persis-

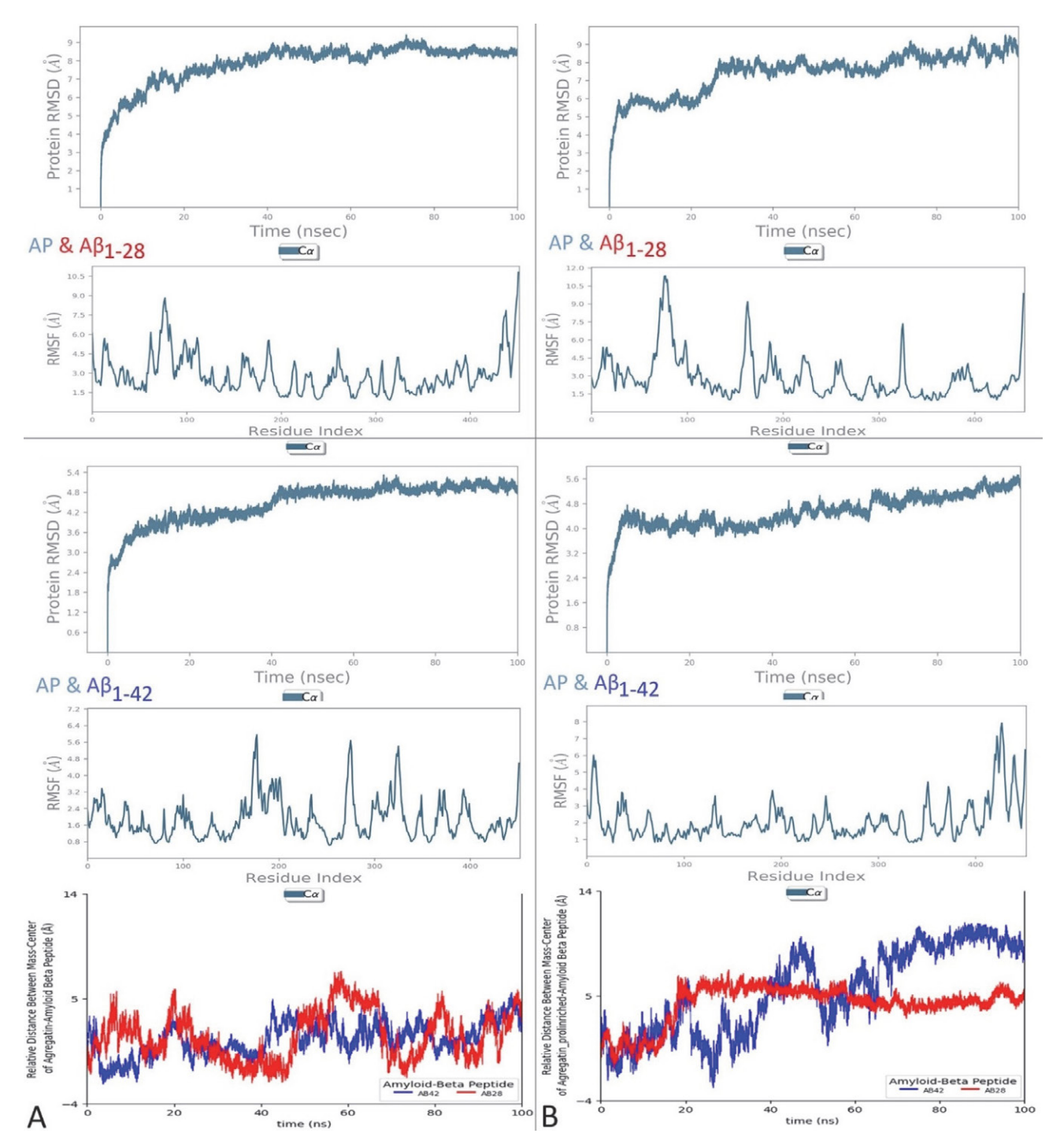


Figure 7: Dynamic stability of AP-A β complexes monitored over 100 ns MD simulations. (A) Protein RMSD and RMSF plots for AP bound to A β_{1-28} (red) and A β_{1-42} (blue). RMSD trajectories plateau after ~30 ns, indicating global structural stabilization, while RMSF peaks correspond mainly to loop and terminal regions. (B) Center-of-mass (COM) distance analyses. Left: overall COM distances between AP and A β peptides remained within 3-6 Å, confirming stable association. Right: when focusing on the proline-rich domain of AP, A β_{1-28} maintained a compact and stable interaction (~5 Å), whereas A β_{1-42} displayed larger fluctuations and drifted beyond 8 Å after ~60 ns, consistent with its higher flexibility. AP: Aggregatin protein, A β : Amyloid-beta peptide, COM: center-of-mass.

tent interface with the PRD, whereas the longer $A\beta_{1-42}$ peptide exhibits more dynamic binding, consistent with its higher flexibility observed in RMSF analyses.

The reported RMSD and RMSF values provide detailed insights into the structural behavior of AP-A β com-

plexes across the 100 ns simulations. RMSD trajectories increased during the initial 20–30 ns but subsequently plateaued in the 3.0–5.5 Å range, indicating conformational convergence without evidence of large-scale unfolding. This stabilization suggests that the complexes reached

equilibrium within the early phase of the simulations. RMSF profiles further revealed that the largest fluctuations were confined to terminal loop regions and solvent-exposed domains, which are inherently flexible, whereas the binding interfaces between AP and A β exhibited consistently low fluctuations (typically 2–4 Å). These findings demonstrate that the interaction interfaces remained intact and conformationally rigid. Notably, A β _{1–42} complexes displayed moderately higher flexibility relative to A β _{1–28}, which aligns with the longer peptide chain length and its well-documented propensity for aggregation. Taken together, these results support that the modeled AP-A β interactions maintain structural integrity under physiological-like conditions and likely reflect biologically relevant binding modes.

Previous experimental evidence has pointed to the role of AP in facilitating A β aggregation, and the MD simulations provide a mechanistic explanation for how this might occur at the molecular level. Specifically, the strong hydrogen bonds and salt bridges interactions between AP and A β suggest that AP may act as a scaffold that stabilizes intermediate A β oligomers, promoting further aggregation into toxic fibrillar forms. This is particularly relevant because it aligns with the hypothesis that early-stage A β oligomers are more neurotoxic than mature fibrils, reinforcing our confidence in the validity of our research.

MD simulations offer a computational approach to study protein-peptide interactions at an atomic level. This report focuses on MD simulations to explore the interactions between AP and AB peptides, offering insights into binding mechanisms, stability, and potential therapeutic implications. The goal is to identify key interaction residues, structural conformational changes, and energy profiles of the complex formation. As illustrated in Figure 1, based on earlier research, persuasive evidence suggests that the transition of $A\beta$ from the α -helix to the β -sheet structure dramatically hastens the formation of aggregates.^{29–31} Our observation that A β peptides in the β -sheet form can readily interact with the AP not only promotes but also expedites the formation of aggregates, thus emphasizing the profound implications of our research. Interestingly, we found that the binding energy with AP and the transformed $Aβ_{1-28, 1-42}$ (converted to β-sheet form) is higher than that of the interaction of AP and standard $A\beta_{1-28, 1-42}$ peptides (see Figure 7 A and B). More notably, the Aβ peptides underwent a dynamic transformation from α -helix to β -sheet structure, significantly enhancing the accuracy of predicting their formation with AP. This transformation process is a key aspect of our research, demonstrating the dynamic nature of biochemistry and neuroscience.

The in vitro studies have affirmed their presence in the nerve cells' plasma membrane, nucleoplasm, Golgi apparatus, cell junctions, Midbody ring, and mitochondria. Moreover, our preceding paper ascertained that AP exhibits a meaningful cell membrane position. More importantly, our analysis uncovered that AP includes a pro-

line-rich region (147-299 aa). Proline-rich proteins (PRPs), abundant in sheep colostrum, are known for their role in immune modulation and potential neuroprotective benefits, particularly in neurodegenerative diseases. These proteins have revealed potential in improving cognitive abilities in both animal studies and patients with AD. 18 Regarding this, we hypothesized that the results would produce superior docking scores compared to generating NMR structures for $A\beta_{1-42}$ and $A\beta_{1-28}$. In particular, separate simulation experiments were conducted with $A\beta_{1-42}$ and $A\beta_{1-28}$ in the AP proline-rich region, showing that $A\beta_{1-42}$ displaces from the AP throughout the simulation while $A\beta_{1-28}$ is exhibited more stable behavior, as seen in Figure 7B. This observation is consistent with the RMSD/ RMSF analyses, where the higher RMSD values in $A\beta_{1-42}$ trajectories reflected enhanced flexibility in loop and C-terminal regions rather than disruption of the binding interface. This outcome may be because exclusively the G38 residue of $A\beta_{1-42}$ forms hydrogen bonds with the A175 residue of AP, while $A\beta_{1-28}$ interacts with AP using multiple strong bonds, such as hydrogen and salt bridges (see Supplementary file 2). H13, K28, Q15, and S8 of Aβ (N-terminal region) through two simulations were found to interact with charged residues in AP, forming hydrogen bonds and salt bridges that contributed to the overall stability of the complex. Noteworthily, of these residues, H13 and K28 are capable of contacting multiple residues in the AP, and the binding potential of residue H13 reached 100% over 100 ns. Structural representations of the complexes (Figure 6) illustrate these interactions, showing that H13, K16, and K28 of Aβ form stable hydrogen bonds with AP residues P185, G186, and N195, corroborating the trajectory-based interaction data. Both simulation results suggest that AP plays a significant role in promoting the aggregation of Aβ peptides. By forming stable interactions with critical regions of Aβ, mainly N-terminal regions such as residues 1-27^{10,32}, AP potentially might accelerate the formation of amyloid fibrils. The binding of AP to these regions may enhance the nucleation process of Aβ, a critical early step in amyloid fibril formation. Plus, the residues such as K16, L17, and E22 in the Aβ peptide were involved in hydrophobic interactions with AP. Besides, detailed residue-level interactions between AP and AB peptides were analyzed and summarized in Supplementary File 2. Several recurrent contacts were observed, particularly hydrogen bonds involving AP residues A176, A179, N300, and N330 with $A\beta_{1-28}$ residues such as H6, S8, and E3. Among these, the A176-S8 and N330-backbone interactions showed high occupancy over the simulation timeframe, persisting for more than 30% of the trajectory duration. In addition, highly persistent contacts such as AP D252-Aβ H13 (100% occupancy), AP D415-Aβ V12 (98.6%), and AP R323-Aβ E3 (72.9%) (see Supplementary file 2) further confirm that the PRD interface remains conformationally stable even in trajectories with elevated RMSD values. These residues may represent key interaction hotspots contributing to the observed stability of the complexes and suggest localized affinity regions on the proline-rich surface of AP.

Interestingly, the MD simulations did not reveal significant structural destabilization or unfolding of the AP protein upon binding to A β peptides. This indicates that the binding event does not lead to significant conformational changes in AP, supporting the hypothesis that it may serve as a stabilizing scaffold for A β peptides during the aggregation process. This conformational stability is crucial for AP's role in facilitating amyloid fibril formation because it suggests that the protein remains functional and stable while promoting A β aggregation.

The observation that only minor shifts in β -sheet regions near the binding site occur upon interaction with $A\beta$ peptides suggests that AP is structurally well-suited to accommodate amyloidogenic peptides. This raises the question of whether the protein itself could be targeted to disrupt its interaction with $A\beta$, potentially inhibiting the aggregation process at an early stage.

The findings from these MD simulations have significant implications for therapeutic strategies aimed at preventing or reducing amyloid plaque formation in AD. Targeting the interaction between AP and A β peptides could offer a novel therapeutic approach. Small molecules or peptides that disrupt fundamental hydrophobic or electrostatic interactions between AP and A β could serve as potential inhibitors of amyloid fibril formation.

Furthermore, the stable interaction interface identified in the MD simulations provides valuable information for structure-based drug design. The hydrophobic pockets and charged residues that mediate AP-AB binding could be targeted by rationally designed inhibitors that block the initial nucleation and aggregation steps of A\(\beta\). These inhibitors could reduce the formation of toxic Aβ oligomers, thereby slowing the progression of AD. Regarding this, Abdulraheem and Durdagi investigated as a first attempt to find inhibitors targeting the AP by screening FDA-improved drugs with a computer drug design approach.¹¹ According to their findings, the inhibitors they investigated showed significant interactions with the residues ALA108, ARG319, GLN9, GLN14, and LEU250 of AP with Cefpiramide, and SER245 and TYR244 of AP with Diniprofylline, indicating that these residues are critical for ligand binding.11 Using three different tools, we found that among the alternative docking results, $A\beta_{1-42}$ interacted with the ARG319 residue of AP.10 These findings highlight the critical role of the ARG319 residue in ligand binding to AP, as evidenced by the interactions of both Cefpiramide and $A\beta_{1-42}$ with this key residue.

AP plaques and amyloid accumulations in AD patients and numerous APP transgenic mice indicate the pressing need to understand and control the unregulated function of AP, depending on its genetic interconnection with A β . In this regard, after strong evidence is clear, various biological tests can provide valuable knowledge of the

role and therapeutic potential of the AP as a target for AD. These tests encompass cell-compartment analysis to explore the functional results of AP or its interaction with A β -peptide. Establishing the cellular origin of the AP will be a significant step in forthcoming studies. This could potentially open up a new avenue of hope in the fight against AD, as it will be crucial to determining whether AP could be a viable therapeutic target. Just as A β peptides stem from the APP protein in the cell membrane and play a role in aggregation and plaque formation alongside the AP outside the cell, AP could also originate from the cell membrane.

Interestingly, the MD simulations did not reveal significant structural destabilization or unfolding of the AP protein upon binding to A β peptides. This indicates that the binding event does not lead to significant conformational changes in AP, supporting the hypothesis that it may serve as a stabilizing scaffold for A β peptides during the aggregation process. This conformational stability is crucial for AP's role in facilitating amyloid fibril formation because it suggests that the protein remains functional and stable while promoting A β aggregation.

The observation that only minor shifts in β -sheet regions near the binding site occur upon interaction with $A\beta$ peptides suggests that AP is structurally well-suited to accommodate amyloidogenic peptides. This raises the question of whether the protein itself could be targeted to disrupt its interaction with $A\beta$, potentially inhibiting the aggregation process at an early stage.

3. 3. Limitations and Future Directions

While MD simulations provide crucial insights into the molecular interactions between AP and Aβ peptides, several challenges remain. First, longer simulation times and more extensive system sizes could further clarify the dynamics of amyloid fibril formation in the presence of AP. Second, the influence of post-translational modifications (such as phosphorylation or glycosylation) on AP's interaction with AB remains fully understood and should be addressed in future studies. Moreover, it would be essential to validate the MD simulation results through experimental methods, including X-ray crystallography, cryo-EM (cryo-electron microscopy), or nuclear magnetic resonance (NMR), or to confirm the binding sites and interaction patterns observed in silico. The other limitation of the present study is the 100 ns duration used for each MD simulation. While this timeframe allows for the assessment of local structural stability and comparative binding behavior across multiple docking poses, it may not fully capture slower conformational transitions or rare binding rearrangements. Simulations were run for several independent AP-AB complexes based on diverse docking poses, thereby partially addressing sampling variability. However, future studies should consider extending simulations to 500 ns or 1 µs for at least one representative complex to explore longer-timescale events. Additionally, metrics such as hydrogen bond lifetimes or center-of-mass distances could be monitored to evaluate convergence and interaction dynamics over extended periods. Finally, in vivo studies are needed to assess the pathological relevance of the AP-A β interaction and test potential inhibitors' efficacy in preventing amyloid aggregation and AD progression.

4. Conclusion

In summary, MD simulations of the interaction between AP and A β - provide compelling evidence that AP is critical in promoting amyloid aggregation. The detailed insights into molecular interactions and binding stability offer a promising foundation for the development of therapeutic interventions aimed at disrupting this interaction, potentially slowing or preventing the progression of AD. As the understanding of protein-peptide interactions in AD pathology grows, targeting molecular modulators like AP represents a novel and exciting approach in the search for effective AD treatments.

Acknowledgements

Supercomputing resources in this work have been supported by the Plataforma Andaluza de Bioinformatica of the University of Malaga, and by the supercomputing infrastructure of the NLHPC (ECM-02, Powered@NLH-PC).

5. References

- 1. M. A. Busche, B. T. Hyman, *Nat. Neurosci.* **2020**, *23*(10), 1183–1193. **DOI:**10.1038/s41593-020-0687-6
- 2. J. Weller, A. Budson, *F1000Res.* **2018**, *7*, 1–9. **DOI**:10.12688/f1000research.14506.1
- 3. S. Y. Tan, M. B. Pepys, P. N. Hawkins, *Am. J. kidney Dis.* **1995**, *26* (2), 267–285. **DOI**:10.1016/0272-6386(95)90647-9
- K. Zou, D. Kim, A. Kakio, K. Byun, J.-S. Gong, J. Kim, M. Kim, N. Sawamura, S. Nishimoto, K. Matsuzaki, B. Lee, K. Yanagisawa, M. Michikawa, *J. Neurochem.* 2003, 87(3), 609–619. DOI:10.1046/j.1471-4159.2003.02018.x
- J. Hardy, D. J. Selkoe, Science. 2002, 297(5580), 353–356.
 DOI:10.1126/science.1072994
- S. H. Chong, S. Ham, Phys. Chem. Chem. Phys. 2012, 14(5), 1573–1575. DOI:10.1039/C2CP23326F
- T. Zhang, J. Zhang, P. Derreumaux, Y. Mu, J. Phys. Chem. B 2013, 117(15), 3993–4002. DOI:10.1021/jp312573y
- 8. Y. Chebaro, P. Jiang, T. Zang, Y. Mu, P. H. Nguyen, N. Mousseau, P. Derreumaux, *J. Phys. Chem. B* **2012**, *116*(29), 8412–8422. **DOI:**10.1021/jp2118778
- T. Yan, J. Liang, J. Gao, L. Wang, H. Fujioka, X. Zhu, X. Wang, Nat. Commun. 2020, 11(1), 1–16.
 DOI:10.1038/s41467-019-13962-0

- N. Besli, G. Yenmis, Acta Chim. Slov. 2020, 67(4), 1262–1272.
 DOI:10.17344/acsi.2020.6175
- Z. T. J. Alabdulraheem, S. Durdagi, J. Mol. Graph. Model. 2023, 125, 108575. DOI:10.1016/j.jmgm.2023.108575
- 12. D. T. Jones, *J. Mol. Biol.* **1999**, *292*(2), 195–202. **DOI:**10.1006/jmbi.1999.3091
- Y. Song, F. DiMaio, R. Y.-R. Wang, D. Kim, C. Miles, T. J. Brunette, J. Thompson, D. Baker, *Structure* 2013, 21(10), 1735–1742. DOI:10.1016/j.str.2013.08.005
- G. C. P. Van Zundert, J. Rodrigues, M. Trellet, C. Schmitz, P. L. Kastritis, E. Karaca, A. S. J. Melquiond, M. van Dijk, S. J. De Vries, A. Bonvin, *J. Mol. Biol.* 2016, 428(4), 720–725.
 DOI:10.1016/j.jmb.2015.09.014
- O. Trott, A. J. Olson, J. Comput. Chem. 2010, 31(2), 455–461.
 DOI:10.1002/jcc.21334
- E. F. Pettersen, T. D. Goddard, C. C. Huang, G. S. Couch, D. M. Greenblatt, E. C. Meng, T. E. Ferrin, *J. Comput. Chem.* 2004, 25(13), 1605–1612. DOI:10.1002/jcc.20084
- S. J. De Vries, M. Van Dijk, A. M. J. J. Bonvin, *Nat. Protoc.* 2010, 5(5), 883. DOI:10.1038/nprot.2010.32
- A. Gladkevich, F. Bosker, J. Korf, K. Yenkoyan, H. Vahradyan, M. Aghajanov, *Prog. Neuro-Psychopharmacology Biol. Psychiatry.* 2007, 31(7), 1347–1355.
 DOI:10.1016/j.pnpbp.2007.06.005
- K. Tsujikawa, K. Hamanaka, Y. Riku, Y. Hattori, N. Hara, Y. Iguchi, S. Ishigaki, A. Hashizume, S. Miyatake, S. Mitsuhashi, Y. Miyazaki, M. Kataoka, L. Jiayi, K. Yasui, S. Kuru, H. Koike, K. Kobayashi, N. Sahara, N. Ozaki, M. Yoshida, A. Kakita, Y. Saito, Y. Iwasaki, A. Miyashita, T. Iwatsubo, T. Ikeuchi, T. Miyata, G. Sobue, N. Matsumoto, K. Sahashi, M. Katsuno, Sci. Adv. 2022, 8(21), eabm5029. DOI:10.1126/sciadv.abm5029
- Schrödinger Release, Desmond Molecular Dynamics System, Maest. Interoperability Tools, Schrödinger, New York, NY 2017.
- 21. R. Pawara, I. Ahmad, S. Surana, H. Patel, *Silico Pharmacol*. **2021**, *9*(1), 54. **DOI**:10.1007/s40203-021-00113-x
- S. Nosé, Mol. Phys. 1984, 52(2), 255–268.
 DOI:10.1080/00268978400101201
- 23. W. G. Hoover, *Phys. Rev. A* **1985**, *31*(3), 1695. **DOI:**10.1103/PhysRevA.31.1695
- G. J. Martyna, D. J. Tobias, M. L. J. Klein, Chem. Phys. 1994, 101(5), 4177–4189. DOI:10.1063/1.467468
- K. Roos, C. Wu, W. Damm, M. Reboul, J. M. Stevenson, C. Lu, M. K. Dahlgren, S. Mondal, W. Chen, L. Wang, R. Abel, R. A. Friesner, E. D. Harder, *J. Chem. Theory Comput.* 2019, 15(3), 1863–1874. DOI:10.1021/acs.jctc.8b01026
- J. Satoh, Y. Kino, M. Yanaizu, T. Ishida, Y. Saito, *Intractable Rare Dis. Res.* 2020, 9(4), 217221.
 DOI:10.5582/irdr.2020.03080
- A. M. Waterhouse, J. B. Procter, D. M. A. Martin, M. Clamp, G. J. Barton, *Bioinformatics* 2009, 25(9), 1189–1191.
 DOI:10.1093/bioinformatics/btp033
- 28. U. Consortium, *Nucleic Acids Res.* **2019**, 47(D1), D506–D515. **DOI:**10.1093/nar/gky1049
- T. C. T. Michaels, D. Qian, A. Šarić, M. Vendruscolo, S. Linse,
 T. P. J. Knowles, *Nat. Rev. Phys.* **2023**, 5(7), 379–397.

DOI:10.1038/s42254-023-00598-9

S. G. Itoh, H. Okumura, *Int. J. Mol. Sci.* 2021, 22(4), 1859.
 DOI:10.3390/ijms22041859

31. H.-L. Chiang, C.-J. Chen, H. Okumura, C.-K. Hu, J. Comput.

Chem. 2014, 35(19), 1430–1437. DOI:10.1002/jcc.23633
32. J.-M. Shi, H.-Y. Li, H. Liu, L. Zhu, Y.-B. Guo, J. Pei, H. An, Y.-S. Li, S.-D. Li, Z.-Y. Zhang, Y. Zheng, ACS Omega 2022, 7(43), 38847–38855. DOI:10.1021/acsomega.2c04583

Povzetek

Alzheimerjeva bolezen, nevrološka motnja z vse večjo razširjenostjo po svetu, predstavlja velik izziv za medicinsko skupnost. Molekularni mehanizem, ki je osnova njene nevropatologije, še vedno ni v celoti pojasnjen. Nedavne raziskave so se osredotočile na vlogo proteina agregatin (AP), ki ga kodira gen FAM222A, pri agregaciji amiloid-beta (A β) preko njegove N-terminalne A β -vezavne domene. Naša študija si prizadeva opredeliti mehanizme interakcije med AP in A β (1-42 in 1-28) peptidi z uporabo molekularnih dinamičnih (MD) simulacij na atomski ravni. Cilj je oceniti, ali AP deluje kot stabilizacijska matrica pri agregaciji A β peptidov, potrditi rezultate molekularnega sidranja iz prejšnjih raziskav ter primerjati stabilnost in interakcijske profile različnih izoform A β . A β (1-42, 1-28) peptidi so bili pretvorjeni iz α -vijačne v β -listnato obliko, da bi omogočili boljše tvorjenje kompleksov z AP. Izbrane pozicije sidranja iz naše prejšnje raziskave in štiri najbolje ocenjene iz programa HADDOCK so bile vključene v MD simulacije, kar je privedlo do razmeroma stabilnih kompleksov, kot kažejo konsistentni trendi RMSD/RMSF, brez večjih strukturnih motenj. Vendar analiza proste vezavne energije in interakcij ni bila izvedena, zato so zaključki omejeni na opazovanja strukturne stabilnosti. Naši izračuni predstavljajo zanesljivo izhodišče za nadaljnje eksperimentalne raziskave Alzheimerjeve bolezni, usmerjene v načrtovanje in razvoj relevantnih interakcij med proteini in peptidi.



Except when otherwise noted, articles in this journal are published under the terms and conditions of the Creative Commons Attribution 4.0 International License